Remote Sensing of Environment 140 (2014) 107–117

Contents lists available at ScienceDirect

Remote Sensing of Environment

journal homepage: www.elsevier.com/locate/rse

Estimation of soil surface roughness of agricultural soils using airborne LiDAR

Russell Turner [a,b], Rocco Panciera [a,*], Mihai A. Tanase [a], Kim Lowell [a], Jorg M. Hacker [c], Jeffrey P. Walker [d]

[a] Cooperative Research Centre for Spatial Information (CRCSI), University of Melbourne, Australia
[b] Remote Census, NSW, Australia
[c] Airborne Research Australia, School of the Environment, Flinders University, Australia
[d] Department of Civil Engineering, Monash University, Australia

ARTICLE INFO

Article history:
Received 27 March 2013
Received in revised form 22 August 2013
Accepted 22 August 2013
Available online xxxx

Keywords:
LiDAR
Surface roughness
Remote sensing
Airborne

ABSTRACT

Soil Surface Roughness (SR) provides a representation of surface variability which can be an important factor in a range of modelling applications such as surface water flow and sediment/nutrient transport. Moreover, it is a crucial parameter for interpreting backscatter characteristics of Synthetic Aperture Radar (SAR) for agricultural application such as near-surface soil moisture retrieval. SR is typically estimated using manual profiles of height variation along short transects (1 to 3 m). However, this approach can be very time consuming and often only a small number of transects can be measured in this way, which may not be adequate to characterize the spatial variability of SR across the landscape. This study investigated the feasibility of utilising airborne Light Detection and Ranging (LiDAR) observations as an alternative for mapping SR attributes across an agricultural environment in New South Wales, Australia. To that end, SR attributes were extracted from airborne LiDAR observations and compared with those extracted from an extensive ground survey of SR making use of manual pin-profilers. Results show that LiDAR-estimates of soil profile surface heights Root Mean Square (RMS) are both accurate (compared to manual profiles) and precise (repeatable stable estimates) for fields presenting bare or fallow conditions and either presenting no row structure or as long as the orientation of the LiDAR scan line is perpendicular to the row structure. In such cases results indicated a strong correlation between LiDAR-estimated and ground-measured RMS estimates ($R^2 > 0.68$, $p < 0.05$), with an RMSE better than 0.81 cm and bias smaller than 0.48 cm from a 400 m flight altitude. Moreover, estimates produced from repeat pass LiDAR datasets were consistent and highly correlated (R^2 0.98) suggesting that the approach is precise and robust, provided that key tillage parameters (i.e. presence of vegetative material and row direction) can be pre-classified. LiDAR estimates of surface height RMS were shown to be accurate enough to allow the tracking of temporal changes in surface roughness due to farming activities. In contrast, LiDAR-derived surface Correlation Length (CL) estimates were not found to be a reliable proxy of the ground-measured CL.

1. Introduction

Surface roughness (SR) parameters are utilised in a range of applications including sediment and nutrient transport models, and surface water flow (Govers, Takken, & Helming, 2000; Hollaus, Aubrecht, Höfle, Steinnocher, & Wagner, 2011). They are also important when interpreting the backscatter characteristics of Synthetic Aperture Radar (SAR) as with increasing roughness, more of the incident energy is scattered away from the specular direction, resulting in higher backscattering coefficients (Ulaby, Moore, & Fung, 1986). Since this effect competes with that of other variables of interest, such as near-surface soil moisture and vegetation biomass, the knowledge of SR is crucial for the estimation of such variables from SAR observations.

Soil geometry can be categorised into small, medium and large scale parameters (Beadoin, Le Toan, & Gwyn, 1990). At a small scale, the spatial arrangement of individual soil clods (or aggregated clumps) is inherently random. The degree of random SR will vary depending on factors such as the prevailing soil type, the initial cultivation intensity, interaction with vegetation cover and progressive weathering from rain and wind. Medium scale parameters pertain to periodic SR that results from the mechanised and systematic tillage of the soil to create row structure (or periodic pattern) and are usually characterized by alternating raised beds and low furrows to improve the natural drainage properties of the soil (Beadoin et al., 1990). SR in relatively flat uncultivated soils tends to be isotropic, while tilled soils exhibit anisotropic characteristics where SR is directionally dependent on row structure. Small scale random SR can be found in all soils while medium scale periodic SR is only present in cultivated fields. Large scale SR, on the other hand, refers to terrain level characteristics such as slope, elevation and aspect.

* Corresponding author at: CRC for Spatial Information, PO Box 672, Carlton South, VIC 3053, Australia. Tel.: +61 3 83445628; fax: +61 3 9654 6515.
E-mail address: panr@unimelb.edu.au (R. Panciera).

0034-4257/$ – see front matter.
http://dx.doi.org/10.1016/j.rse.2013.08.030

SR geometry is often defined by soil height profiles that are typically expressed in terms of 3 parameters: Root Mean Square (RMS) of surface heights, profile Correlation Length (CL) and profile autocorrelation function, under the assumption that SR can be represented by a single-scale stationary process. These parameters are usually measured using a range of manual techniques including spray boards, squared boards (i.e., mesh board), 3D photogrammetric modelling, pin-profilers or terrestrial laser line profilers (Blaes & Defourny, 2008; Huang & Bradford, 1992; Merel & Farres, 1998; Zribi et al., 2000). However, such methods are labour-intensive. Logistically it is also problematic to cover the full range in soil profile variation across large areas particularly when there is row structure (Blaes & Defourny, 2008). In particular, localised ground measurements of height variation show little spatial dependency, meaning that parameters measured at one position are generally poorly representative of their surroundings (Álvarez-Mozos, Verhoest, Larrañaga, Casalí, & González-Audícana, 2009). The major problems associated with SR parameterization are (1) its scale dependency and (2) its spatial variability (Verhoest et al., 2008). Several studies making use of in-situ, photogrammetric and ground-based LiDAR techniques observed elevated SR spatial variability at the scale of agricultural fields. Álvarez-Mozos et al. (2009) observed coefficients of variation for field-average RMS and CL of respectively 16 to 25% and 38 to 94% depending on the tillage state. Blaes and Defourny (2008) showed that SR parameters calculated along short transects can be highly variable even over small distances, with the RMS and CL varying significantly, from 1.2 to 2.2 cm and from 10 to 70 cm respectively when 1 cm spaced profiles were shifted by 3.5 m in ploughed surface. Similarly, Mattia, Toan, Souyris, et al. (1997) observed values of RMS differing by as much as 4 cm within the same tilled wheat field in southern Italy.

Another problem is related to the scale of observation. A number of studies have shown that natural surfaces are often better described using random fractals rather than stationary single scale processes (Burrough, 1981; Davidson et al., 2000; Zhixiong, Nan, Perdok, & Hoogmoed, 2005), in which case the values of the SR parameters are highly dependent on the profile length used (Mattia et al., 2003; Ogilvy, 1988; Oh & Kay, 1998). For example, Zhixiong et al. (2005) reported an overall increase in RMS by a factor of 1.2 to 1.4 when comparing data obtained from 5-m profiles with those derived from 0.5-m profiles. Oh and Kay (1998) showed that profiles of at least 40 times the CL are needed in order to obtain the RMS with a precision of $\pm 10\%$. Such observation scales are obviously difficult to achieve using ground-based methods. Several studies have reported measurements of surface roughness by means of laser profilers, which measure the distance between a horizontally positioned rail, on which the carriage with the laser beam moves, and the soil surface (Davidson at al., 1998; Davidson et al., 2000; Manninen, 2003; Mattia et al., 2003; Álvarez-Mozos et al., 2009). However, only Mattia et al. (2003) compared the SR parameters derived from the laser profiler with pin-profiler measurements, reporting a good agreement (relative error less than 8%), between CL estimates derived from pin-profilers and laser profilers. For surface height variances, the parameters estimated using a pin-profiler lead to only a slight overestimation for relatively smooth soils. However, ground laser profilers are characterized by a very fine sampling resolution, from 0.1 to 0.5 mm in the vertical direction and 0.1 and 2 mm in the horizontal direction, therefore a reasonable match with pin-profilers is expected.

Other studies have addressed the use of airborne LiDAR (Light Detection and Ranging) measurements for more rapid and cost-effective ways of assessing soil surface structure at the landscape scale (Davenport, Holden, & Gurney, 2004; Hollaus et al., 2011; Kurtz et al., 2003). The commercial availability of airborne LiDAR technology offers a strong potential to economically and efficiently characterize SR spatial distribution over large areas. LiDAR provides a 3D cloud of point based on measuring the return time of a laser pulse emitted from an aerial platform toward the ground. In theory, if acquired at a sufficient sampling density, it should be possible for Airborne Laser Scanners (ALS) to characterize the spatial distribution of SR with high density, high precision elevation measurements that can be rapidly collected over large areas. Both Hollaus et al. (2011) and Kurtz et al. (2003) made use of LiDAR data to estimate roughness of respectively forested areas and sea ice. However, both studies were concerned with meso-scale SR (i.e., spatial scale of decimetres to metres), including roughness of the vegetation layer and ice topographic variation, larger than the centimetre-scale roughness typical of agricultural fields, which is the topic of the present study. Davenport et al. (2004) dealt with such roughness scale in the context of a feasibility study conducted using a helicopter-mounted ALS. It was shown that, although the absolute vertical accuracy of airborne laser altimetry elevation measurement is of the order of 20 cm, relative height measurements can be made with a greater degree of accuracy than might be expected (Davenport et al., 2004). For points collected at very small intervals (50 ms) the only source of surface height uncertainty was the internal noise associated with electronics and the inertial navigation system (INS) corrections. This resulted in a relative surface height accuracy of 3.5 cm as opposed to 20 cm (Davenport et al., 2004). The data density available was not high enough to obtain a reliable figure below the 50 ms time lag. Based on these observations, Davenport et al. (2004) estimated the surface heights RMS at 26 sites distributed over 4 test fields characterized by different cultivation treatments (rolled, harrowed, ploughed and potato-ridged with peak-trough height of respectively 1, 3, 5 and 20 cm). Although no quantitative comparison with ground measurements was performed, results showed that LiDAR observations were able to distinguish between rolled and harrowed fields correctly in 56.9% of the cases, between rolled sites and ploughed fields in 92.5% of the cases, and that the potato-ridged field was distinguished correctly from all other types in 100.0% of cases.

The objective of this study is to expand on the work of Davenport et al. (2004) and quantitatively evaluate the accuracy of high precision airborne LiDAR data (discrete return) to map multiple SR attributed (including surface heights RMS and also CL) over several bare agricultural soils with variable tillage conditions. The study focused on two main questions:

- Can airborne LiDAR accurately retrieve key SR metrics over bare surfaces?
- Are these estimates consistent (precise) in terms of repeat measurements from multiple overpasses during the same mission (i.e. run swath overlaps) and with temporal datasets (17 days apart)?

The study makes use of two airborne surveys conducted with a Riegl LMS-Q560 full-waveform 2D laser scanner together with ground measurements of surface profiles (3-m long) collected over 13 agricultural fields in South-Eastern Australia. The results demonstrate the feasibility of extracting accurate estimates of SR using airborne LiDAR with the potential to implement larger and more cost-effective sampling programs in the future, once the LiDAR acquisition and processing costs will decrease.

2. Study area

The Coleambally Irrigation Area (CIA) is an irrigated agricultural zone in South-East Australia with principal summer crops of rice, soybeans, and maize (corn), winter crops of wheat, oats and barley and pasture for grazing. A 1965 ha study area with over 72 agricultural fields (Fig. 1) was selected in an area of intensive irrigated cropping approximately 45 km west of the town of Narrandera (NSW, Australia). The site location (Latitude: −34° 43′, Longitude: 146°5′) was considered to be representative of the local farming area with mainly flat terrain, a mean elevation of 120 m, predominantly granodiorite soils and an annual rainfall of approximately 419 mm. A range of crop types including wheat, canola and native pasture were present at the time of ground and LiDAR datasets acquisition. The study area is

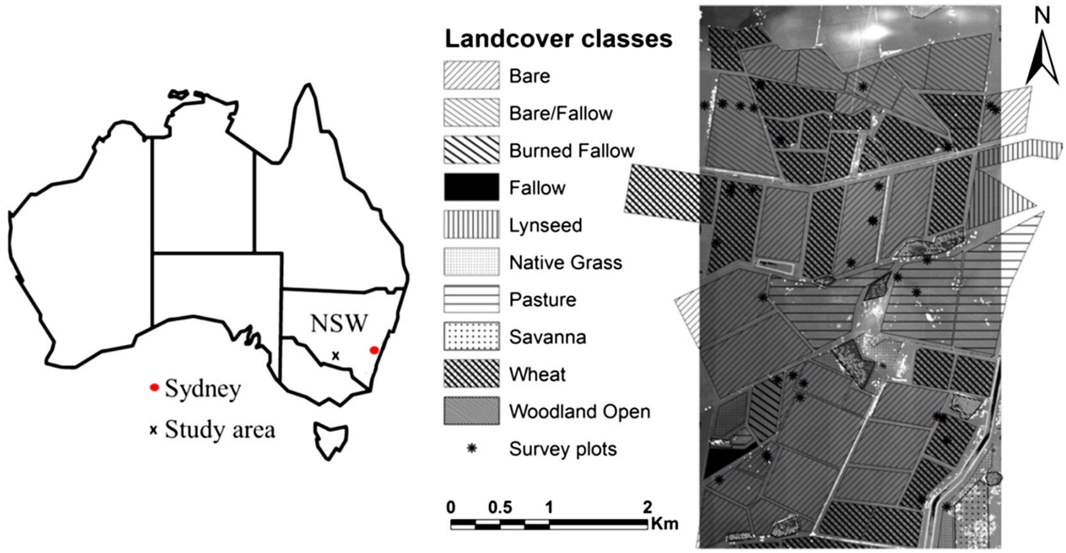

Fig. 1. (a) Map of Australia showing the location of the study area, and (b) a landcover stratification map with the location of the survey plot overlaid on LiDAR-derived elevation map rasterized from point-cloud data.

part of the 36 km × 38 km "Yanco" site which has been intensively monitored for remote sensing purposes since 2001 (Merlin et al., 2008; Panciera et al., 2008; Smith et al., 2012). All data used in this study were collected in the context of the Soil Moisture Active Passive Experiment 3 (SMAPEx-3, 5–23 September 2011, Panciera et al., 2013), an airborne experiment for acquisition of active and passive microwave data to support algorithm development of NASA's SMAP mission.

3. Methodology

3.1. Field survey

An initial field inspection was undertaken to classify the condition of the agricultural fields within the study area. Fields were classified into various land cover classes based on vegetation cover type tillage state and row structure (Fig. 1). Of the 72 agricultural paddocks present in the area, the 13 used in this study were bare soils or fallow (i.e., sparse stubble) for which ground measurements of SR and LiDAR coverage were collected during the field campaign.

Within these 13 bare soil paddocks, a total of 20 survey plot locations (hereby referred to as "plots") were selected for characterizing SR attributes. The plots were distributed to cover the range of tillage conditions encountered in the area, with typically between 1–3 plots for each paddock. Each plot was located using a handheld GPS receiver. The accuracy of the handheld GPS geolocation was tested prior to data acquisition against high precision differential GPS and found to be better than 10 m (RMSE).

At each plot SR attributes were estimated both qualitatively in terms of row structure presence and direction and quantitatively by means of a pin-profiler. This instrument consisted of a 1-m long frame with 0.5 cm spaced vertical pins (Fig. 2). Profile data along transects were recorded using a digital camera. A special mount ensured that the camera lens was always at a fixed distance (1.5 m) and orientation (parallel to the profiler) from the profiler. Once the profiler was put into place the pins were slowly released until they came into contact with the soil surface. A photo of the pin positions was then captured with the digital camera and subsequently an image post-processing software was used to extract the profile from each photograph using the upper red portion of the vertical pins as a reference. At each of the 20 plots profile measurements were repeated three times both along and across row benches, or alternatively in the north–south/east–west direction in the absence of a row structure. Prior to extracting SR attributes, the surface heights measurements from each of the 3, 1-m long profiles were referred to a common reference system, by referencing each 1-m profile to the same horizontal reference plane (i.e., de-trending for local topographic slope) and by eliminating any vertical shift at the overlap between adjacent profiles. This resulted in two perpendicular profiles, each of 3 m in length, equivalent to what would be measured with a 3-m long pin-profiler.

At the end of the post-processing stage a number of key structural parameters were summarised for each plot including: (i) RMS of surface heights, (ii) profile CL, and (iii) periodic structure direction. Moreover, information on farming activities of tillage/ploughing that occurred at each plot during the observation period was gathered through visual observations and by a survey of the local farmers.

For the purpose of this analysis only plots with either completely bare conditions or a limited amount of dead dry biomass were considered. A preliminary analysis showed that plots containing any other type of vegetation (e.g. wheat, or pasture) exhibited poor correlations with LiDAR estimates compared to plots that were either bare earth or fallow (mostly bare). Normally, vegetative material does not present a problem for manual pin-profilers as the operator can manoeuvre the pins between stalks and leaves to measure the soil surface. However, for an airborne LiDAR approach, such material is highly problematic as LiDAR profiles will also contain crop debris in the point cloud data and this can be hard to separate during the post-classification of return points into ground and non-ground classes, particularly for vegetation whose height is less than 50 cm. Moreover, crop vegetation and stubble debris can also mask the soil surface and therefore adversely influence the SR measurements (Blaes & Defourny, 2008). Table 1 summarises the characteristics and the measured SR parameters of the plots used in this study.

3.2. LiDAR data

Airborne LiDAR data were acquired on the 5th and 22nd of September 2011 using a Riegl LMS-Q560 full-waveform 2D laser scanner operated by Flinders University's Airborne Research Australia (ARA), South Australia. The fixed-wing research aircraft was flown at a ground speed of approximately 40 m/s at a nominal altitude of 400 m above the ground along parallel N–S-oriented lines 150 m apart. This resulted in a

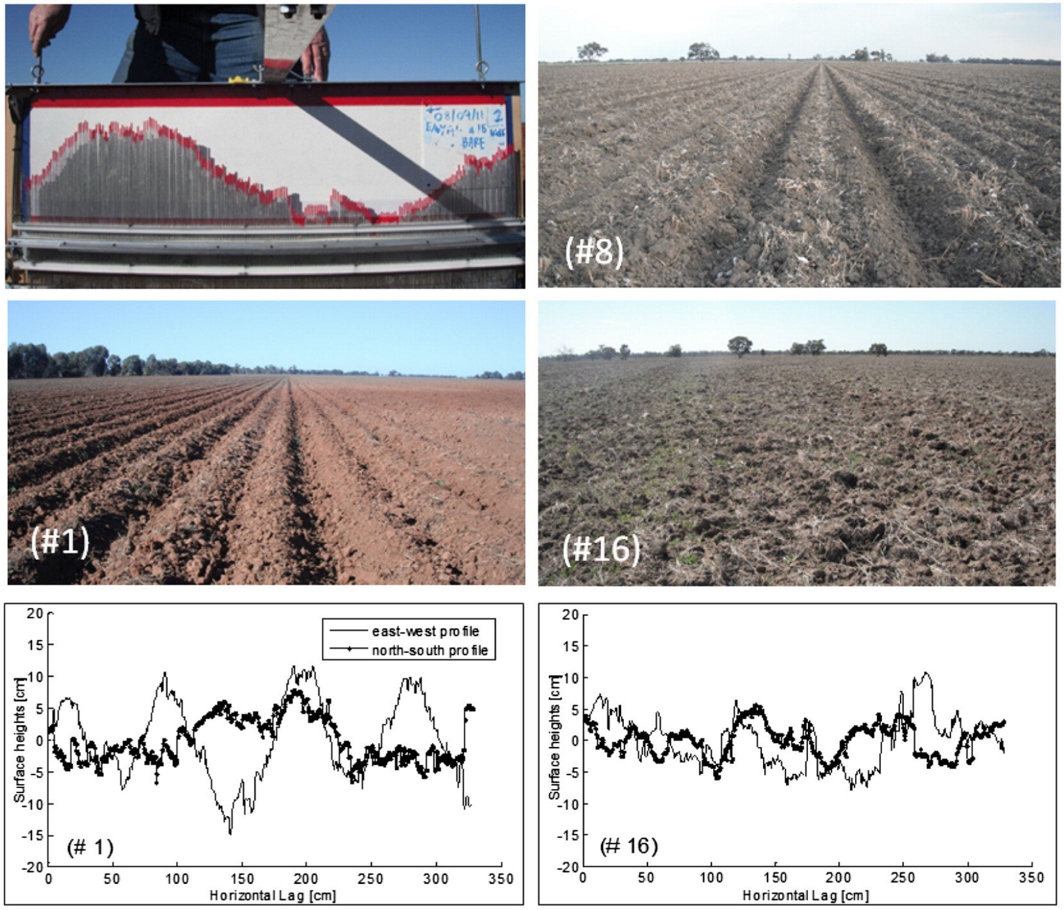

Fig. 2. Photos of the pin-profiler used to characterize surface roughness (top left) and example photos of the plot sampled: (#1) Bare soil with periodic row structure, (#8) Sparse stubble with periodic row structure and (#16) Isotropic surface. Refer to Table 1 for the plot #.

swath width of 340 m with 50% overlap. The laser scanner was configured at a rate of 240 KHz and a maximum scan angle of 22.5°. According to the specifications of the Q560 LiDAR (Riegl, 2006) stating a maximum laser beam divergence of <= 0.5 mrad, this gave a mean ground footprint with a diameter of approximately 20 cm. However, discussions with the manufacturer confirmed (Riegl, personal communication) that this is a worst case value and that the actual ground footprint is probably closer to 12–15 cm. The point spacing was found to be approximately 20 cm (along-track) and 50 cm (across-track) which means that there is only a marginal overlap between individual footprints. Overall, this provided a mean point density of 6 pulses per square metre in parallel scanning lines around 50 cm apart, and postings approximately 20 cm along each scan line. The mission was repeated on the 22nd of September 2011 to check for temporal changes in surface conditions across the area.

Although the flight-line direction (alternate north–south) remained consistent for both missions the row direction within the fields varied across the study area. Consequently, LiDAR scans were a mixture of perpendicular (running across the benches), oblique (running across the benches at an angle) or parallel (running along the benches either on bench-tops or tractor wheel furrows). To address this issue, the survey plots were grouped according to the relative orientation between LiDAR scan line and crop row direction (Table 1). The direction of the LiDAR scan line was east–west (90° from north) for all runs. Given the relatively low aircraft speed (40 m/s) and low flight altitude (400 m) the aircraft heading was fairly stable, resulting in a minimal standard deviation of scan line direction of $\pm 3°$.

Processed LiDAR point data was available in LAS file format with each file representing a north–south strip of data (6.5 km × 340 m), hereby referred to as a "run". The data from each run was analysed separately to avoid any potential geo-registration issues with overlapping swaths which could increase the vertical uncertainty.

3.3. Data processing

A preliminary inspection of the LiDAR point cloud data sets showed subtle anomalies in geo-registration between adjacent runs (approximately 1–2 m in planimetric shift and 14 cm in vertical shift) which could potentially be critical at the fine scale required for estimating SR attributes. LiDAR scan overlaps were not manually adjusted to remove any spatial matching errors particularly with elevation values at swath edges. Rather than introduce additional human error by realigning swath overlaps, run datasets were instead analysed individually over each plot (i.e., extraction of SR parameters was done on data from individual runs, without mixing data points from different runs). Given the high swath overlap (40 to 50%), most plots were covered by 2 to 3 run passes which enabled a comparison of SR estimates from repeat plot scans in the same mission.

In order to calculate SR attributes from LiDAR data for each survey plot, the following procedure was followed. Firstly, all LiDAR points within a 30 m radius of each plot were extracted and associated uniquely to the plot. At this stage points with extreme elevation anomalies were removed from the dataset by calculating a mean point elevation for each plot and deleting points higher than one metre above the mean. This cleaning stage removed a range of high point anomalies that were clearly not associated with the flat terrain such as birds, overhanging tree branches, and overhead power lines. A customised MATLAB program was then used to extract surface profiles from each scan line. Each profile was de-trended to eliminate local topographic slope, which is known to affect the calculation of the roughness

Table 1
Summary of the plot characteristics and ground-measured surface roughness parameters. Where no periodic structure was present, the "Across" and "Along" roughness measurements correspond to the North-South and East-West direction respectively. The "Tilled/ploughed" column indicate: "yes" that the field was either tilled or ploughed between LiDAR acquisition dates; "no" that the field did not undergo any artificial change in surface conditions (by either tillage or ploughing) between LiDAR acquisition dates.

Plot #	Surface type	Row to scanline angle (°)	Row spatial period/depth [cm]	Tilled/ploughed	Scan-to-row orient.	Measured roughness parameters			
						Across rows		Along rows	
						RMS[cm]	CL [cm]	RMS[cm]	CL [cm]
1	Bare	80 (±3)	89/17	no	Perpend.	6.3	16.8	3.5	31.4
2	Bare	80 (±3)	89/17	no	Perpend.	7.0	18.8	2.0	11.5
3	Bare	80 (±3)	89/17	no	Perpend.	6.9	18.8	1.6	8.9
4	Bare	80 (±3)	86/18	no	Perpend.	7.0	17.5	1.6	6.7
5	Bare	70 (±3)	193/21	yes	Perpend.	6.6	22.3	1.1	2.6
6	Bare	80 (±3)	193/21	no	Perpend.	4.2	19.8	2.5	11.2
7	Sparse stubble	80 (±3)	184/13	yes	Perpend.	5.7	22.5	1.7	5.7
8	Sparse stubble	80 (±3)	176/18	no	Perpend.	4.6	13.5	2.3	10.0
9	Bare	50 (±3)	265/7	yes	oblique	3.3	11.0	5.1	30.8
10	Sparse stubble	10 (±3)	182/19	yes	Parallel	7.0	23.5	3.0	4.8
11	Sparse stubble	10 (±3)	182/19	yes	Parallel	6.5	21.6	1.5	5.3
12	Sparse stubble	10 (±3)	182/19	yes	Parallel	5.6	24.0	2.3	13.9
13	Sparse stubble	10 (±3)	224/29	yes	Parallel	9.1	26.8	2.7	3.1
14	Bare	20 (±3)	196/20	no	Parallel	7.6	23.6	1.5	10.8
15	Sparse stubble	0 (±3)	89/17	no	Parallel	3.3	18.7	0.8	2.3
16	Sparse stubble	none	–	yes	Isotropic	1.2	15.6	0.5	9.9
17	Sparse stubble	none	–	no	Isotropic	2.7	9.7	1.5	8.8
18	Sparse stubble	none	–	no	Isotropic	5.0	30.3	4.2	11.3
19	Sparse stubble	none	–	no	Isotropic	4.1	34.0	4.2	17.4
20	Sparse stubble	none	–	yes	Isotropic	2.7	5.7	3.3	22.5

parameters. Surface profiles were extracted from each scan line with a length of 3 m to match the length of the ground manual profiles. Furthermore all scan lines within 10 m of the plot centre were considered to accommodate the expected positional error of the GPS coordinates as well as the relative planimetric shift between adjacent LiDAR runs. The surface heights RMS and the profile CL were then calculated for each profile. This procedure ensured that SR parameters were calculated using only relative LiDAR heights measured along the same LiDAR scan line over a 3-m length. As shown by Davenport et al. (2004), over time lags smaller than 50 ms the only source of surface height uncertainty is the internal noise associated with electronics and the inertial navigation system (INS) corrections. At the 240-KHz rate of the LiDAR system available in this study, the time lag between subsequent LiDAR points along a scan line was of 4 μs, which translated into a time lag between all the data points over a 3-m LiDAR profile not superior to ~50 μs. This is largely within the 50 ms figures indicated by Davenport et al. (2004) to allow the detection of centimetre-scale roughness.

A plot-average value and associated standard deviation of the RMS and CL were finally assigned to each plot by averaging the RMS and CL calculated for each individual scan line falling within 10 m from the location of the pin-profiler. This procedure was chosen to characterize the spatial variation of SR at the plot scale and also to compensate for planimetric errors in the geolocation of LiDAR points (1–2 m planimetric accuracy) and survey plots (10 m planimetric accuracy). The number of scan lines per plot varied greatly, between approximately 30 and 130 with an average of 80 scan lines per plot, with small values indicating only partial plot coverage for the specific swath. In order to exclude such cases from the analysis, a threshold on the minimum number of LiDAR points was set at 75% of the average number of points per plot. Swaths with the number of points below this value were removed from the analysis of each plot.

3.4. Surface roughness parameters calculation

The computation of the surface heights RMS and profile CL was done using the same MATLAB routine applied to both the ground and LiDAR profiles. Given a profile formed of a sequence of N data points with surface height z_i with respect to a reference plain, then RMS is defined as:

$$\mathrm{RMS} = \sqrt{\frac{1}{N}\sum (z_i - \mu)^2}, \quad (1)$$

where μ is the average of z_i over the profile length. For the calculation of the CL, first the empirical autocorrelation function (ACF) was calculated for each individual profile (each LiDAR scan line and each ground profile). A mathematical function was then fitted to the empirical ACF. For this task, three functions were considered which have been commonly shown to fit well the ACF of agricultural surfaces: Exponential, Gaussian and hybrid (fractal) (Baghdadi et al., 2004):

$$\rho(x) = e^{-\left(\frac{x}{L}\right)} \quad : \text{Exponential} \quad (2)$$

$$\rho(x) = e^{-\left(\frac{x}{L}\right)^2} \quad : \text{Gaussian} \quad (3)$$

$$\rho(x) = e^{-\left(\frac{x}{L}\right)^\tau} \quad : \text{fractal} \quad (4)$$

where $\rho(x)$ is the surface correlation function at the horizontal spatial lag x and $\tau = -1.67\,D + 3.67$ is the fractal dimension, which is approximately 1.4 for agricultural plots (Baghdadi et al., 2004). Thus, the coefficient τ is approximately 1.33.

For each profile the most suitable ACF fitting function was selected as the one providing the minimum root mean square error between theoretical and empirical ACF (such automated procedure was necessary since, due to the large number of LiDAR profiles, it was impractical to visually fit each individual empirical ACF). In the case of the LiDAR-derived profile, the exponential function was the best fit in 52% of the cases, while the Gaussian and fractal where the best fit in respectively the 38% and 10% of the cases. Conversely, for the ground profiles the Gaussian function was the best fit in 50% of cases, followed by the exponential (30%) and fractal (8%). This is a result of the coarser sampling resolution of the LiDAR data (20 cm) with respect to the ground profiles (0.5 cm), which results in a more abrupt decrease in correlation for small lags typical of the exponential function. A few examples of empirical and fitted ACF can be found in Fig. 4.

Once a suitable mathematical function is found to fit the empirical ACF, the correlation length is calculated as the fitting parameter L in Eq. ((2)–(4)), equivalent to spatial lag x at which the ACF is equal to $1/e$. It should be noted that no frequency decomposition was performed on the surface profiles, i.e., the surface heights RMS and profile CL calculated include both high-frequency roughness variations due to soil clods and surface irregularities as well as low-frequency variations due to crop rows.

4. Results and discussion

Data analysis focused on four main areas:

1. Impact of the spatial sampling spacing on the calculation of SR parameters;
2. A comparison between field survey and LiDAR SR estimates;
3. A comparison between LiDAR SR estimates from scan overlaps in the same mission, and
4. A comparison between LiDAR SR estimates between dates (17 days apart).

In the following sections the results for each main area listed above are presented, followed by an overview of potential sources of error.

4.1. Impact of spatial sampling spacing on surface roughness parameters

The LiDAR and pin-profiler are different sampling methods, generally characterized by different spatial sampling spacing (20 cm and 0.5 cm respectively in the case of this study) and different length of the profile sampled. Since the objective of this paper is to cross-compare the SR statistical parameters derived from the two sampling methods, it is crucial to understand how the difference in sampling parameters (spacing and profile length) between the two methods affects the calculation of the SR parameters. Although generally the total length of the profile sampled would be different between the two sampling methods, in this study this was avoided by extracting LiDAR profiles with the same length as the ground profiles (3 m). Therefore in this section we limit the analysis to the impact of different sampling spacing. The surface heights RMS and CL estimated with the pin-profiler can be thought of characterizing the micro- (e.g. millimetres to decimetres) spatial scale. This is associated to surface irregularities such as soil clods. Conversely, LiDAR-derived estimates are likely to capture the meso- (e.g. decimetres to metres) spatial scale associated to local topographic variations as well as periodic structures resulting from man-made farming activities (see Fig. 4). As shown in Table 1, the spatial periods of the periodic row structures were in the 89–224 cm range, with depths varying from 7 to 20 cm. In order to understand the effect of the sampling spacing on the calculation of the SR parameters, a synthetic analysis was conducted as follows: each 0.5 cm-spaced profile measured with the pin-profiler at the plots listed in Table 1 was segmented at the LiDAR sampling spacing (20 cm). In order to simulate the integration of the energy distribution within LiDAR footprints, the average pin-profiler reading within each 20 cm segment was then taken. A sub-sampled profile was then constructed using such averages. Up to 40 sub-sampled profiles were extracted from each original profile, each shifted of 0.5 cm. The surface roughness RMS and CL were then calculated for all profiles as explained in Section 4.4. Such sub-sampled profiles can be thought as close proxies of the profiles which would be observed by the LiDAR sensor with a 20 cm footprint. However, they are not affected by the LiDAR measurement error, nor errors associated to the co-geolocation of LiDAR and pin-profiler. Therefore the comparison between the SR parameters calculated on the original and sub-sampled profiles provide a direct insight into the effect of the sampling spacing on the SR parameters. Fig. 3 shows such comparison. For each profile, the average and standard deviation of the roughness parameters (surface heights RMS and CL) calculated on the 40 sub-sampled (20 cm spacing) profiles is compared with the roughness parameters derived from the original (0.5 cm spacing) profile.

The main observation to be drawn from Fig. 3 is that the simulated LiDAR estimates of surface heights RMS are strongly correlated with that of the original profile ($r^2 = 0.98$). However, the coarser sampling spacing introduced a small negative bias (underestimation) of -0.5 cm (± 0.3 cm error standard deviation), fairly uniform across the range of RMS and across surface types. This underestimation is consistent with that observed in previous studies (Ogilvy & Foster, 1989). Conversely, the retrieval of CL is more significantly affected by the coarser sampling spacing, and this is highly dependent on the surface type. While the mean overestimation error is fairly small for “perpendicular” (2.4 ± 0.7 cm) plots, it rises to 7.4 ± 2.3 cm for “parallel” and 7.7 ± 1.5 cm for “isotropic” plots, with a maximum overestimation of 20 cm in some cases. This is accompanied by a larger variation in CL extracted from the sub-sampled profiles (vertical error bars in Fig. 3b). This is quite unexpected, since the spatial period and trench depths of the crop rows are very similar for “parallel” and “perpendicular” plots (see Table 1), and therefore one would expect the sampling spacing to have the same impact on the CL calculation, regardless of the relative direction between the crop rows and the LiDAR scan line.

To understand the reason for such a difference, in Fig. 4 examples of surface profile and associated ACF are shown for each surface type. All profiles present a high-frequency component (noise associated to soil clods) superimposed to a low-frequency pattern (due to local topographic slope variation for the “parallel” and “isotropic” fields and to the

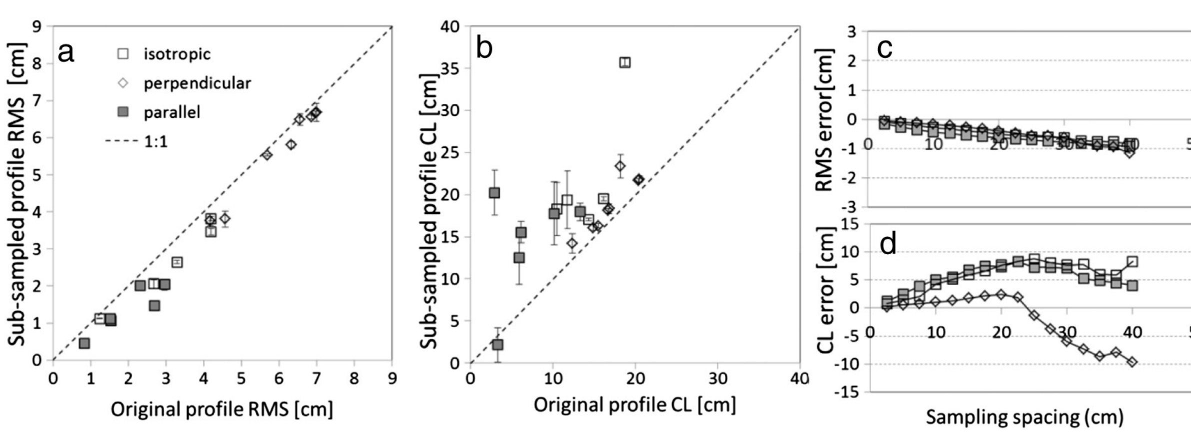

Fig. 3. Impact of profile sampling spacing on the retrieval of surface roughness parameter. Comparison between surface heights RMS (a) and CL (b) derived from synthetic profiles created by sub-sampling at 20 cm spacing original profiles at 0.5 cm sampling spacing. (c–d) Dependence of the average error in surface heights RMS (c) and CL (d) between sub-sampled and original profiles. All vertical error bars represent the standard deviation of the error across the synthetic profiles.

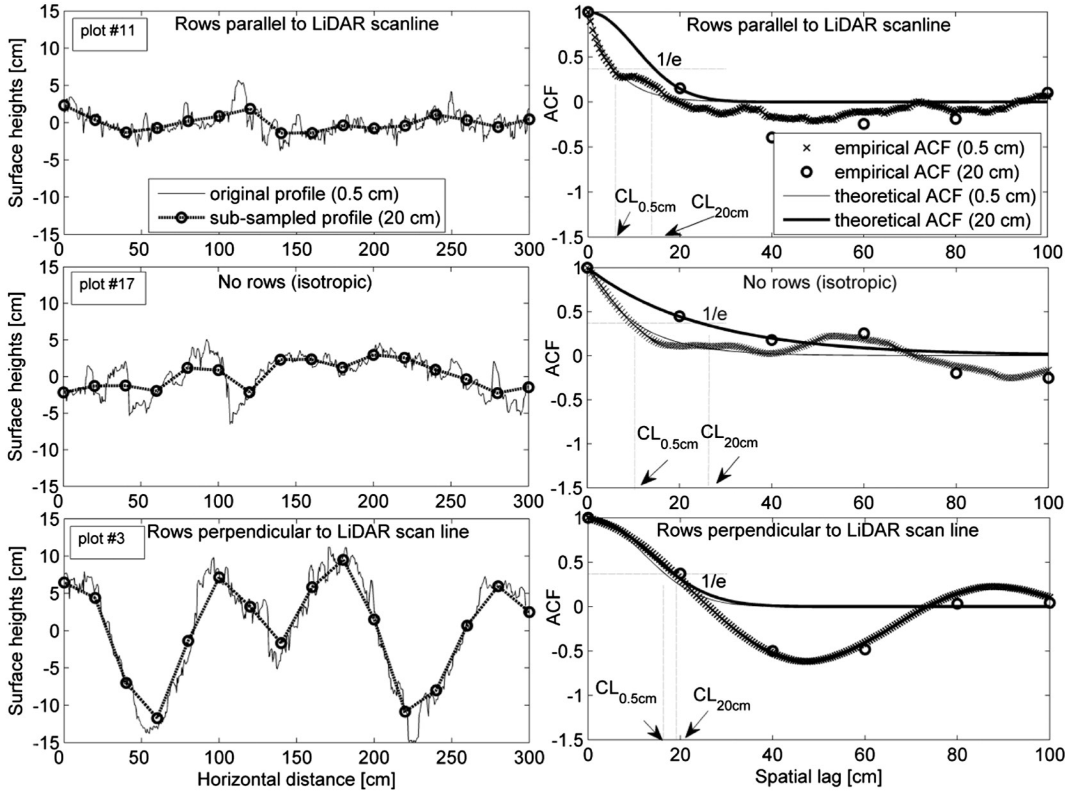

Fig. 4. (left panels) Examples of 0.5 cm-spaced surface profiles and 20 cm-spaced sub-sampled profiles and (right panels) empirical and fitted theoretical autocorrelation function (ACF) for both profiles. In the right panels the correlation lengths derived from the theoretical ACF for the 0.5 cm-spaced profile ($CL_{0.5cm}$) and 20 cm-spaced profile (CL_{20cm}) are also shown. Plot # cross-references to Table 1.

periodic row structure for the "perpendicular" plots). In the case of the "perpendicular" plots the experimental ACF from original and sub-sampled profiles are very similar and capture the decorrelation component associated to the low-frequency pattern, resulting in a good match of the CL calculated from original and sub-sampled profiles. Conversely, for "parallel" and "isotropic" plots the ACF derived from 20 cm sub-sampled profiles do not capture the decorrelation component at small lags associated to the high-frequency noise, which is instead reflected in the original ACF, resulting in a larger CL (i.e., flatter surface) for the sub-sampled profiles and explaining the overestimation observed in Fig. 3b. For completeness, in Fig. 3c and d the variation of surface heights RMS and CL error (i.e., difference in RMS and CL relatively to a 0.5 cm-spaced profile) with increasing sampling spacing are shown for spacings up to 40 cm. The underestimation of RMS increased nearly linearly with increasing sampling spacing, up to −1 cm for 40 cm spacing. The error in CL exhibits a different behaviour depending on the surface type. For "parallel" and "isotropic" type profiles, characterized by rather low values of RMS and the absence of a periodic roughness component associated to row structure, (see Fig. 4), the CL extracted from sub-sampled profiles increasingly overestimates the CL extracted from 0.5 cm profiles as the spacing increases. Conversely, for surfaces characterized by a periodic roughness component and elevated surface heights RMS ("perpendicular" profiles), the difference in CL remains small, increasing to only 2 cm, up to 20 cm sampling spacing (approximately 1/3 of the spatial periods for perpendicular surfaces, see Table 1), after which the original CL is strongly underestimated.

The synthetic analysis has therefore shown that, despite the difference in sampling spacing, LiDAR observations at 20 cm spacing have the potential to provide estimates of surface heights RMS matching those derived from ground pin-profiler observations within a mean error of 0.5 cm (±0.3 cm) for all surface types analysed. In terms of CL, the coarser sampling spacing of the LiDAR is expected to introduce negligible errors for surfaces presenting a periodic surface pattern associated to crop rows when the surface is scanned by the LiDAR in the direction perpendicular to the periodic structure. Conversely, for plots without a periodic surface pattern (either isotropic plots or plots scanned by the LiDAR in the direction approximately parallel to the crop rows) CL could be overestimated between 10 and 20 cm due to the LiDAR coarse sampling spacing. In the next section the comparison between airborne LiDAR and ground pin-profiler roughness estimates is performed.

4.2. Comparison between ground survey and LiDAR surface roughness estimates

Fig. 5 shows the scatter plots between LiDAR- and field-derived estimates of RMS and CL. The accuracy of the LiDAR estimates exhibited a strong dependence to the relative direction between crop rows and LiDAR scan direction. A good agreement between LiDAR and ground estimates of RMS was observed for both plots with crop rows perpendicular to the LiDAR scan line (RMSE 0.77 cm, bias 0.48 cm and R^2 0.76) and for isotropic plots (RMSE 0.81 cm, bias 0.03 cm and R^2 0.68), confirming the feasibility of estimating surface height RMS with airborne LiDAR at least for bare fields having such surface conditions. Conversely, the accuracy of LiDAR estimates of RMS decreased significantly when the crop row direction was oblique or approximately parallel to the LiDAR scan direction, with an increase in RMSE of up to 4.1 cm and a 3.8 cm positive bias (overestimation). The reason for such higher estimates of surface heights RMS on "parallel" plots is unclear. However, it was observed that the vertical range of LiDAR heights recorded on such plots is consistent with the depth of the benches (~20 cm, see Table 1). This suggests that, when LiDAR scan lines and crop rows are approximately parallel, LiDAR footprints along the scan line might be recording elevations of the bottom and top of the row benches, probably due to unavoidable deviation of the crop row from a straight line or the effect of the surface height variation

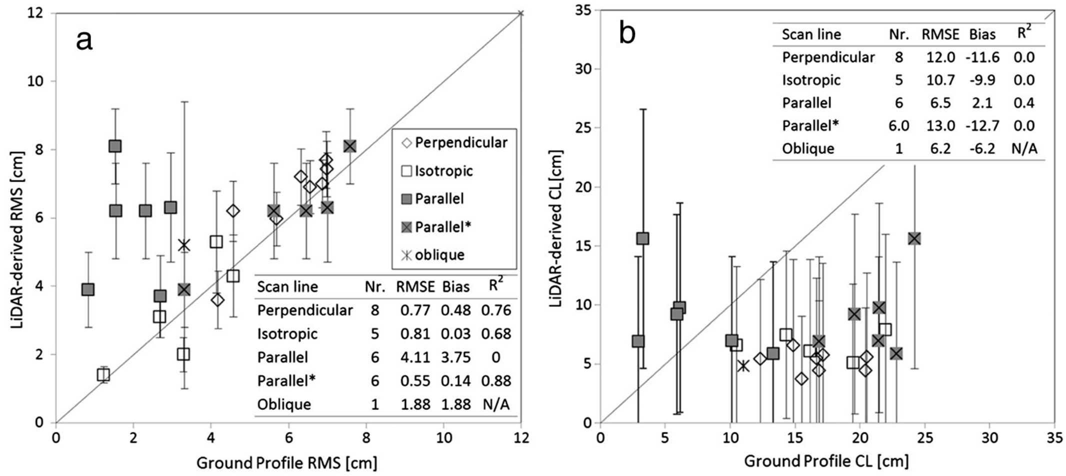

Fig. 5. Relationship between ground-based pin-profiler estimates of (a) RMS and (b) CL and those derived from airborne LiDAR for bare soil plots. Vertical error bars indicate ±1 standard deviation of the RMS derived from individual scan lines within 10 m of each plot. Data points and error metrics in the tables are grouped by relative direction between crop rows and LiDAR scan lines (see Table 1). 'Parallel*' indicate comparison between LiDAR scan line parallel to the crop row direction with pin-profiler measurements perpendicular to the crop row direction.

within the LiDAR footprints when these fall close to the edges of the benches. Since the ground profile was instead accurately positioned along the bottom or top of the benches, and perfectly parallel to the crop rows, it will record a smaller surface heights RMS than the LiDAR. If this is true, then the surface heights RMS derived from LiDAR over a "parallel" plot should better match the RMS of the ground profile measured in the direction perpendicular to the crop rows at the same location, rather than parallel to the crop rows. This is confirmed in Fig. 5 where the LiDAR-extracted RMS was plotted versus the pin-profiler perpendicular to the crop rows. The RMSE in surface heights RMS decreased significantly from 4.1 cm to 0.55 cm, the bias and correlation improving accordingly, indicating that, even when the LiDAR scan lines are approximately parallel to the direction of the periodic structures, the LiDAR-derived RMS is a precise estimate of the RMS as measured across the crop rows.

LiDAR estimates of CL were generally poor and not correlated with those estimated from ground profiles. CL was generally largely underestimated by the LiDAR profiles, up to −11.6 cm bias in the worst case of crop rows perpendicular to the LiDAR scan line. As for the case of surface heights RMS estimates, on "parallel" plots the LiDAR CL estimates were generally higher than for "perpendicular", "isotropic" or "oblique" plots, particularly for plots presenting small values of CL for the ground profiles, and could overestimate the ground profile CL by up to 15 cm. For such plots LiDAR CL estimates were also highly variable in the surroundings of the ground profile (see large vertical error bars in Fig. 5 for "parallel" crops). Such overestimation is somewhat consistent with what was observed in Section 4.1 for "parallel" plots, where an overestimation of up to 10–20 cm was shown to be associated to the LiDAR coarse sampling spacing.

However, the general underestimation of CL seen in Fig. 5b for "perpendicular", "isotropic" and "parallel" plots at higher values of ground profile CL does not reflect what is expected from the synthetic analysis of Section 4.1. Other sources of error might be at play in this case. The fact that a strong underestimation of CL is observed for larger values of ground CL points to the fact that the sampled profiles (3 m) might be too short to allow for a robust and stable estimate of the CL, which would then remain largely affected by random errors, as suggested by Oh and Kay (1998). Moreover, as noted in previous studies (Álvarez-Mozos et al., 2009; Blaes & Defourny, 2008) CL exhibits higher spatial variability than RMS at both the local (within metres) and paddock scales, and this would undermine the representativeness of the CL estimates derived from the single ground transect of the surrounding 10 m area sampled by the LiDAR. Whether it is the insufficient length of the profile or the local spatial variability that determines the large error bars observed in Fig. 5b is difficult to determine. Although profiles longer than 3 m could be extracted from the LiDAR scan lines, this would not be to the benefit of the comparison with the ground profile as these were limited to 3 m in length.

It should be stressed that, due to the inherent sparse nature of the ground-measured pin profiles, in this study the comparison had to be done between a single ground profile and several (between 30 and 130) LiDAR-derived profiles measured within 10 m from the location of the ground profile, averaged so as to compensate for errors in relative geolocation between the two. Although in this study the ground profiles are considered the "truth" against which the LiDAR estimates were assessed, the point nature of the ground measurements, together with the known high spatial variability of SR attributed over short distances poses doubts about the validity of such a perspective. It could be argued that the LiDAR estimate, although affected by measurement error, might provide a more reliable local estimate of SR because they characterize the spatial variability in SR, as opposed to the highly localised nature of the ground profile. This problem may be difficult to resolve and ultimately it might be only relevant when related to the observations scale of the phenomena which have to be modelled/analysed using the SR attributes. For example, in SAR backscatter modelling, the ensemble average profile over the SAR pixel (~10 m) is generally used. In that regard, the validity of the present study is to demonstrate that, at least in terms of RMS, the two estimates of SR attributes (LiDAR and ground profiles) are highly correlated and only offset by a modest amount (<0.48 cm).

4.3. Consistency of LiDAR scan overlaps

If airborne LiDAR is to provide a robust approach for SR estimation then it is important to verify sampling precision in addition to the accuracy just demonstrated in the previous section. To demonstrate precision, repeated LiDAR scans over the same plot should yield similar SR values. Because the LiDAR runs in this study were flown with up to 50% swath overlap, and most survey plots were covered by two to three run passes, it was possible to compare LiDAR-derived RMS and CL estimates from repeated plot scans.

Using LiDAR data from all the acquisition dates a total of 67 paired run sets (i.e., same-day overpasses of the same location from different runs) were identified across the existing survey plots. An initial analysis based on all paired plots showed a very high correlation in LiDAR-derived RMS estimates (R^2 0.95, RMSE 0.74 cm). This correlation improved further when the analysis was limited to only bare earth plots (R^2 0.98, RMSE 0.29 cm) as illustrated in Fig. 6. These results

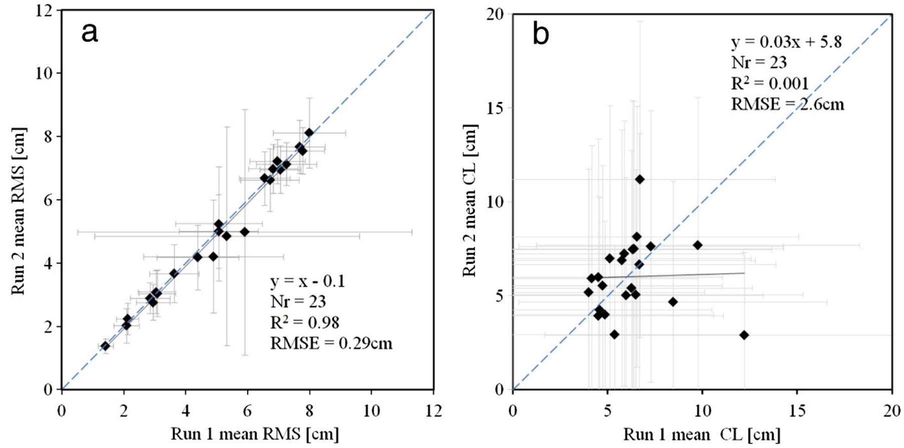

Fig. 6. Comparison of airborne LiDAR-derived RMS (left) and CL (right) estimates of the same location from adjacent runs (bare soil plots only). Vertical error bars indicate ±1 standard deviation of the RMS (and CL) of scan lines within 10 m of each plot. The equation of the regression line, correlation coefficient (R^2) and Root Mean Square Error (RMSE, cm) are also shown.

demonstrate that LiDAR-derived RMS estimates are very stable between subsequent overpasses. Moreover, such a good match between estimates from adjacent overpasses indicates that the impact of the anomalies in LiDAR geo-registration discussed in Section 4.3 is negligible. This consistency between runs suggests that the approach can provide precise and reliable estimates of the RMS.

The repeat pass results for CL estimates were less consistent than the RMS estimates and exhibited no correlation (R^2 0.001). However, overall they provided very similar CL estimates (RMSE 2.6 cm), as shown in Fig. 6. Again, these results may be influenced by the inherently high spatial variability of CL within the 10 m plots. This might be further complicated by slightly different scan directions from repeat passes. The calculation of CL was indeed found to be very sensitive to the relative angle between LiDAR scan and the row direction (see Section 4.2). This is particularly evident as the scan-line direction approaches the row direction, as the LiDAR profile will measure low frequency fluctuations resulting in a higher and more variable value for CL.

Results indicate that airborne LiDAR offers a stable and robust way to estimate RMS values. This consistency between RMS estimates from different runs supports the case that LiDAR-derived RMS estimates are highly stable between adjacent flight lines and that an individual run-based approach is a valid method for analysing point data for SR attributes.

4.4. Temporal consistency of LiDAR data

For this study, LiDAR was acquired on two mission dates (5th and 22nd of September 2011) and this provided an opportunity to assess the consistency in LiDAR SR estimates at different times over the same site. A preliminary analysis of the data showed a significant variation between RMS estimates between the two dates. However, given the stability of LiDAR RMS estimates observed for adjacent runs, it was suspected that much of this variation was actually associated with physical change in surface conditions from mechanical tillage/ploughing events between mission dates. A survey was conducted with local farmers to identify which fields had undergone changes in surface conditions (tillage or ploughing) during the monitoring period (see Table 1). Fig. 7 shows the comparison of LiDAR-derived RMS estimates from the two acquisition dates separately for tilled and untilled plots.

Fig. 7 indicates that LiDAR-derived RMS and CL estimates for fields where no change occurred (i.e. “untilled” fields) were very similar between September 5th and 22nd (R^2 0.99, RMSE 0.23 cm), while those where change had occurred (i.e. “tilled” fields) showed considerable variation of RMS between the two sampling dates. Furthermore, the majority of tilled plots showed a general reduction in RMS that is consistent with the increased mechanical breakdown of soil aggregates.

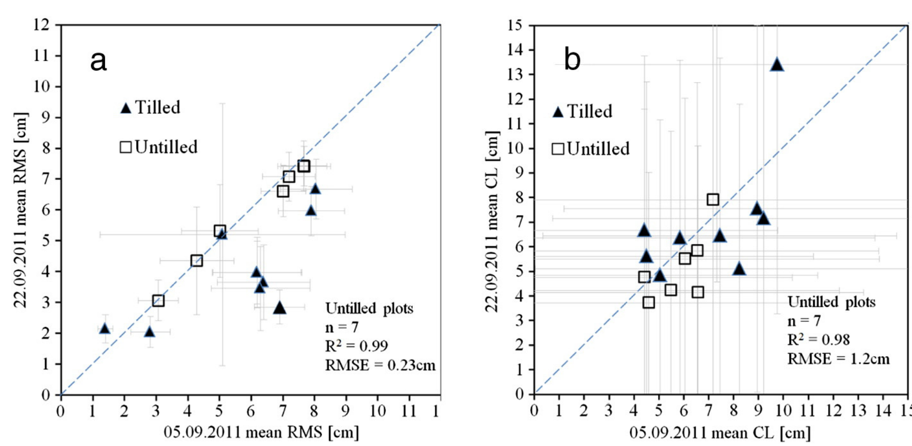

Fig. 7. Comparison of airborne LiDAR-derived (a) RMS and (b) CL estimates of the same locations from different missions (5th and 22nd of September 2011) for bare soil plots. Data points are classified as “tilled” or “untilled” based on the occurrence of physical change in surface conditions from mechanical tillage/ploughing events between mission dates. Vertical error bars indicate ±1 standard deviation of the RMS (and CL) of scan lines within 10 m of each plot.

There are two important points to be made regarding Fig. 7. First, the graph demonstrates the need to separate tilled and untilled plots before comparing LiDAR-derived RMS estimates. Secondly, it appears that variation in LiDAR RMS estimates from temporal datasets may also provide an objective means of tillage change detection. Hence, temporal LiDAR data provides an opportunity to detect changes in tillage treatment over time based on the degree of shift in LiDAR RMS estimates. This observation could provide an innovative and objective means of change detection without the need for ground-based surveys.

Results confirm that LiDAR-derived RMS estimates are consistent between missions over the same plots. Moreover, all bare plots exhibited a very slight decrease in RMS between the 5th and 22nd of September which may have been associated with natural weathering. Interestingly, the LiDAR-derived CL estimates in Fig. 7 also revealed a strong correlation (R^2 0.98, RMSE 1.2 cm) for untilled bare plots with perpendicular scan lines but with a more marked decline in values over time. Again this may have been associated with natural weathering.

4.5. Discussion of potential error sources in LiDAR SR estimates

Various sources of error may have had some degree of influence on the accuracy of the results from this study. These factors include the following:

- *Spatial co-registration* of ground survey and airborne LiDAR data needs to be as accurate as possible to compare datasets over the same location. Unfortunately, co-registration of soil profiles with laser profiles can be problematic. Blaes and Defourny (2008) noted that some of the variation between their terrestrial laser line profiles and photogrammetric DEM estimates was partially due to the difficulty in co-registering their datasets. They state that it was difficult to perfectly match the laser line positions and the soil DEM extracted profiles even though they were captured over the same plot which was clearly marked (via a taped boundary)in the field. In this study, the ground pin-profilers were located using a handheld GPS with relatively low planimetric accuracy (at best a 10 m horizontal accuracy in the x and y plane). In contrast, the spatial accuracy of the airborne LiDAR data was estimated to be within ±50 cm, although a planimetric shift of ~1–2 m between subsequent scans indicate that the spatial accuracy of LiDAR could be on that order of magnitude. Consequently it was not possible to precisely relate the pin-profiler and LiDAR profile datasets at the small scale. To allow for a potential positioning error of ±5 m in the field plot, the LiDAR data were extracted for a 10 m radius around the plot centres in the hope that general trends would appear for both small- and medium-scale parameters. Unfortunately, it was not possible to definitively demonstrate that the manual profiles were actually representative of the larger plot area, although the excellent correlation between ground-derived and LiDAR-based average RMS values is a strong argument in that sense.
- *Spatial resolution* could also be a major source of error. Pin-profilers and LiDAR profilers have different ways of sampling. A pin-profiler can measure height variation in a 2D plane at 0.5 mm intervals, with no sampling overlap along a 3 m transect in two directions (i.e. along the bench and across the bench) and therefore sample points are consistent at set intervals and spacing. In contrast, the airborne LiDAR data in this case were collected within a 3D area with 12–15 cm circular to oblique footprints that are overlapping at inconsistent intervals (approximately 20 cm apart) with variable scan orientation (including perpendicular, oblique and parallel directions). These major differences in how height variation is measured are an obvious source of potential error.
- *Natural weathering* may have occurred between the date of LiDAR acquisition and the ground survey. Although local meteorological records indicate no recorded rain events between these dates, it is possible that wind erosion may have reduced SR.
- *Sensor error* is always a possible source of uncertainty particularly for estimating small scale SR parameters. Official specifications for the Riegl LMS-Q560 (Riegl, 2006) suggest that at an 800 m height the sensor can achieve 7 cm vertical and 19 cm horizontal at 1 sigma (meaning ~68% of the data will fall within this limit). However, these accuracies are based on the assumption that the target is perfectly flat, larger than the beam footprint, and perpendicular to the angle of incidence, none of which hold true for this study. Furthermore, even though the sensor was flown at 400 m above the ground, there is likely to be some unknown degree of vertical inaccuracy which may influence RMS and CL estimates. For example, given the specified range accuracy for the instrument (≤20 mm ±20 ppm), at a distance of 400 m we would expect a range error of around 28 mm.
- *Viewing geometry* can be an important factor when interpreting LiDAR accuracy. LiDAR sensors are not infinite point sampling instruments because the beam width widens the farther it travels. Hence the footprint size and shape will vary according to ground elevation and slope, as well as scan angle in a complex interaction of the transmitted pulse energy with the target. The return signal from a target surface will be a function of the integrated energy distribution across the footprint weighted by the reflectivity profile of the terrain within the footprint. In general, non-uniform targets with differences in reflectivity and slope across the footprint introduce uncertainty in the X, Y and Z position. In our study, the nominal footprint size at ground level was approximately 12–15 cm and in theory this means that a first return could be triggered from up to 7 cm away from the beam centre. This could be an issue particularly at the edges of row benches where height can vary by as much as 20 cm within a distance of 0.5 m. Scan orientation is also an important factor in planning LiDAR acquisition programs. Ideally LiDAR profiles should be extracted perpendicular to the row direction to capture the undulation in row structure. However, since ALS is typically acquired in linear strips using fixed-winged aircraft it is not always possible to achieve a consistent perpendicular scan as different fields exhibit variable row directions. Moreover, row direction can also vary within a field due to slight changes in topography and the presence of physical obstacles (such as paddock trees, rock outcrops, boggy areas, irrigation infrastructure). Consequently, LiDAR soil scans will always contain a mix of optimum and sub-optimum scan directions. Future work should focus on the pre-classification of soil geometry to determine the spatial orientation of rows relative to the viewing geometry of the LiDAR profiles.
- *Point classification* involves the automated separation of ground and non-ground points which can greatly influence the estimation of ground SR parameters. The ability to classify ground from non-ground points is very difficult in agricultural soils, particularly if a periodic row structure is also present. Numerous studies have investigated techniques for filtering and classifying point cloud data (see Meng, Currit, & Zhao, 2010 for a review). Meng et al. (2010) highlighted three feature types for which current ground filtering algorithms are suboptimal and future research is required: surfaces with rough terrain or discontinuous slope, dense forest areas that laser beams cannot penetrate, and regions with low vegetation that is often ignored by ground filters. Because our approach to estimating surface roughness is based on the analysis of individual scan lines, future work should investigate the use of linear neighbourhoods to classify ground points since some studies have shown it to be sensitive to low vegetation (Meng, 2005).

5. Conclusions

The most common method for sampling surface geometry involves labour-intensive field surveys. Airborne laser scanners provide an unprecedented opportunity to efficiently characterize soil SR spatial distribution over large areas. This paper provides the first quantitative assessment against conventional ground-based measurements of the accuracy of airborne LiDAR estimates of surface roughness (surface heights Root Mean Square - RMS, and Correlation Length - CL). The study uses two airborne LiDAR surveys over 13 bare agricultural paddocks in South-Eastern Australia with coincident ground surveys. This paper has demonstrated that despite potential errors from several sources, airborne LiDAR-estimates of the surface height RMS are both accurate (compared to field-derived measurements) and precise (repeatable stable estimates). LiDAR- and field-derived RMS estimates were shown to be highly correlated ($R^2 > 0.68$ and up to 0.88) and accurate (RMSE < 0.81 cm, bias < 0.48 cm). RMS estimates were also shown to be very stable between subsequent overpasses within the same flight mission (R^2 0.98) confirming that the sampling technique is consistent and reliable. The additional benefit of the approach used is that it is independent of the need to manually adjust swath overlaps which can be very time intensive and costly. The temporal change analysis demonstrated that, at least for RMS estimates, airborne LiDAR offers a stable and robust way to measure soil surface roughness over time (i.e. 17 days) with results confirming a very high correlation (R^2 0.99) in repeat RMS estimates across sites where no agricultural activities were recorded during the observation period. Moreover, LiDAR estimates of surface height RMS were shown to be accurate enough to allow the tracking of temporal changes in surface roughness due to farming activities, suggesting that it may be feasible to develop detection methods for the estimation of tillage changes based on shifts in surface height RMS as a surrogate indicator.

This study has also highlighted some major limitations concerning the retrieval of surface roughness parameters from LiDAR. In particular, LiDAR-derived CL estimates were not found to be a reliable proxy of the field-derived CL. The most accurate LiDAR-derived CL estimates, obtained over plots with crop rows parallel to the LiDAR scan direction, produced substantial errors compared to field-derived CL estimates (RMSE 6.5 cm, bias 2.1 cm and R^2 0.4), while for plots with crop row direction perpendicular to the LiDAR scan direction the LiDAR estimates were even more inaccurate (RMSE 12 cm, −11.6 cm bias and R^2 0.0). Such underestimation of the field estimate of CL by the LiDAR could not be entirely explained by the effect of the coarse sampling spacing of the LiDAR alone, as they were generally different in sign than what was expected from the synthetic analysis performed.

The main limitation for the routine application of LiDAR for estimation of RMS is the requirement for information on crop row direction. Therefore, a method to pre-classify the crop row direction is required so that optimum fields and/or flight line direction can be determined. This could be done using optical data or even through analysis of the same LiDAR observations. However, if possible, LiDAR surveys should be carried out at perpendicular bearings to avoid this problem. Moreover, the analysis presented had to be limited to bare surfaces. Sites with vegetation or stubble debris cover would also require improved point cloud classification models to better separate true ground points from elevated noise.

Acknowledgements

This project was funded by an Early Career Researcher grant provided by the University of Melbourne with additional funding from an Australian Research Council (ARC) Super Science Fellowship (FS100100040) and from the Cooperative Research Centre for Spatial Information (CRCSI). The authors would also like to thank Ying Gao and Frank Winston (Department of Civil Engineering, Monash University) for assisting in the collection of the ground data, Andrew McGrath and Wolfgang Lieff at Airborne Research Australia/Flinders university for undertaking the LiDAR flights and Francois Charbonneau and Mélanie Trudel for providing the QuiP digital image processing package.

References

Álvarez-Mozos, J., Verhoest, N. E. C., Larrañaga, A., Casalí, J., & González-Audícana, M. (2009). Influence of surface roughness spatial variability and temporal dynamics on the retrieval of soil moisture from SAR observations. *Sensors*, *9*(1), 463–489.

Baghdadi, N., Gherboudj, I., Zribi, M., Sahebi, M., King, C., & Bonn, F. (2004). Semi-empirical calibration of the IEM backscattering model using radar images and moisture and roughness field measurements. *International Journal of Remote Sensing*, *25*(18), 3593–3623.

Beadoin, A., Le Toan, T., & Gwyn, Q. H. J. (1990). SAR observations and modeling of the C-band backscatter variability due to multi-scale geometry and soil moisture. *IEEE Transactions on Geoscience and Remote Sensing*, *28*(5), 886–895.

Blaes, X., & Defourny, P. (2008). Characterizing bidimensional roughness of agricultural soil surfaces for SAR modeling. *IEEE Transactions on Geoscience and Remote Sensing*, *46*(12), 4050–4061.

Burrough, P. A. (1981). Fractal dimensions of landscapes and other environmental data. *Nature*, *294*.

Davenport, I. J., Holden, N., & Gurney, R. J. (2004). Characterizing errors in airborne laser altimetry data to extract soil roughness. *IEEE Transactions on Geoscience and Remote Sensing*, *42*(10), 2130–2141.

Davidson, M. W. J., Le Toan, T., Mattia, F., Satalino, G., Manninen, T., & Borgeaud, M. (2000). On the characterization of agricultural soil roughness for radar remote sensing studies. *IEEE Transactions on Geoscience and Remote Sensing*, *38*, 630–640.

Davidson, M., Le Toan, T., Maurice Borgeaud, M., & Manninen, T. (1998). Measuring the roughness characteristics of natural surfaces at pixel scales: Moving from 1 meter to 25 meter profiles. *Int. geoscience and remote sensing symp. (IGARSS'98), Seattle, WA*.

Govers, G., Takken, I., & Helming, K. (2000). Soil roughness and overland flow. *Agronomie*, *20*, 131–146.

Hollaus, M., Aubrecht, C., Höfle, B., Steinnocher, K., & Wagner, W. (2011). Roughness mapping on various vertical scales based on full-waveform airborne laser scanning data. *Remote Sensing*, *3*, 503–523.

Huang, C. H., & Bradford, J. M. (1992). Applications of a laser scanner to quantify soil microtopography. *Soil Science Society of America Journal*, *56*(1), 14–21.

Kurtz, N. K., Markus, T., Cavalieri, D. J., Krabill, W., Sonntag, J. G., & Miller, J. (2003). Comparison of ICES at data with airborne laser altimeter measurements over Arctic sea ice. *IEEE Transactions on Geoscience and Remote Sensing*, *46*(7), 1913–1924.

Manninen, A. T. (2003). Multiscale surface roughness description for scattering modelling of bare soil. *Physica A: Statistical Mechanics and its Applications*, *319*, 535–551.

Mattia, J., Davidson, F., Le Toan, M. W. J., D'Haese, T., Verhoest, C. M. F., Gatti, N. E. C., et al. (2003). A comparison between soil roughness statistics used in surface scattering models derived from mechanical and laser profilers. *IEEE Transactions on Geoscience and Remote Sensing*, *41*, 1659–1671.

Mattia, F., Toan, T. L., Souyris, J. -C., De Carolis, G., Floury, N., Posa, F., Member, IEEE, & Pasquariello, G. (1997). The effect of surface roughness on multifrequency polarimetric SAR data. *IEEE Transactions on Geoscience and Remote Sensing*, *35*(4), 954–966.

Meng, X. (2005). A slope- and elevation-based filter to remove non-ground measurements from airborne LIDAR data. *Proceedings of ISPRS WG III/3, III/4, V/3 workshop "laser scanning 2005", The Netherlands* (pp. 23).

Meng, X., Currit, N., & Zhao, K. (2010). Ground filtering algorithms for airborne LiDAR data: A review of critical issues. *Remote Sensing*, *2*, 833–860, http://dx.doi.org/10.3390/rs2030833.

Merel, A. P., & Farres, P. J. (1998). The monitoring of soil surface development using analytical photogrammetry. *The Photogrammetric Record*, *16*(92), 331–345.

Merlin, O., Walker, J. P., Kalma, J. D., Kim, E. J., Hacker, M. J., Panciera, R., Young, R., Summerell, G., Hornbuckle, J., Hafeez, M., & Jackson, T. (2008). The NAFE'06 data set: Towards soil moisture retrieval at intermediate resolution. *Advances in Water Resources*, *31*(11), 1444–1455.

Ogilvy, J. A. (1988). Computer simulation of acoustic wave scattering from rough surfaces. *Journal of Physics D: Applied Physics*, *21*, 260–277.

Ogilvy, J. A., & Foster, J. R. (1989). Rough surfaces: Gaussian or exponential statistics? *Journal of Physics D: Applied Physics*, *22*, 1243–1251.

Oh, Y., & Kay, Y. C. (1998). Condition for precise measurement of soil surface roughness. *IEEE Transactions on Geoscience and Remote Sensing*, *36*, 691–695.

Panciera, R., Walker, J. P., Jackson, T. J., Gray, D. A., Tanase, M. A., Ryu, D., Monerris, A., Yardley, H., Rüdiger, C., Wu, N., Gao, Y., & Hacker, J. M. (2013). The soil moisture active passive experiments (SMAPEx): Towards soil moisture retrieval from the SMAP mission. *IEEE transactions on geoscience and remote sensing*, *51*(99), 1–18, http://dx.doi.org/10.1109/TGRS.2013.2241774.

Panciera, R., Walker, J. P., Kalma, J. D., Kim, E. J., Hacker,, J. M., Merlin, O., Berger, M., & Skou, N. (2008). The NAFE'05/CoSMOS data set: Towards SMOS soil moisture retrieval, downscaling and assimilation. *IEEE Transactions on Geoscience and Remote Sensing*, *46*(3), 736–745.

Riegl (2006). *Airborne laser scanner LMS-Q560 — general description and data interfaces.* User manual. A-3580 Horn, Riedenburgstr. 48, Austria: Riegl Laser Measurement Systems GmbH (135 pp.).

Smith, A.B., Walker, J. P., Western, A. W., Young, R. I., Ellett, K. M., Pipunic, R. C., Grayson, R. B., Siriwardena, L., Chiew, F. H. S., & Richter, H. (2012). The Murrumbidgee soil moisture monitoring network data set. *Water Resources Research*, *48*(7).

Ulaby, F. T., Moore, R. K., & Fung, A. K. (1986). *Microwave remote sensing: Active and passive. Radar Remote Sensing and Surface Scattering and Emission theory*, *Vol. 3*, Dedham, MA: Artech House.

Verhoest, N. E., Lievens, H., Wagner, W., Álvarez-Mozos, J., Moran, M. S., & Mattia, F. (2008). On the soil roughness parameterization problem in soil moisture retrieval of bare surfaces from synthetic aperture radar sensors. *Sensors*, *8*(7), 4213–4248.

Zhixiong, L., Nan, C., Perdok, U.D., & Hoogmoed, W. B. (2005). Characterisation of soil profile roughness. *Biosystems Engineering*, *91*, 369–377.

Zribi, M., Ciarletti, V., Taconet, O., Boissard, P., Chapron, M., & Rabin, B. (2000). Backscattering on soil structure described by plane facets. *International Journal of Remote Sensing*, *21*(1), 137–153.